Ditopic complex formation of the crown-containing 2-styrylbenzothiazole

Yu. V. Fedorov,[a] O. A. Fedorova,[a] E. N. Andryukhina,[a] S. P. Gromov,[a] M. V. Alfimov,[a] L. G. Kuzmina,[b] A. V. Churakov,[b] J. A. K. Howard[c] and J.-J. Aaron*[d]

[a] *Photochemistry Center of Russian Academy of Sciences, Novatorov str. 7a, 117421, Moscow, Russia*
[b] *Institute of General and Inorganic Chemistry, RAS., Leninskii pr. 31, Moscow 117907, Russia*
[c] *Chemistry Department, University of Durham, South Road, Durham, UK DH1 3LE*
[d] *ITODYS, Université Paris 7, CNRS (UMR 7086). 1, Rue Guy de la Brosse, 75005, Paris, France*

Received (in London, UK) 31st May 2002, Accepted 24th September 2002
First published as an Advance Article on the web 20th November 2002

The complex formation of 2-styrylbenzothiazole containing a 15-crown-5 ether fragment with alkaline earth metal cations, proton, Ag^+ and Hg^{2+} was studied by optical and X-ray diffraction methods. The compound is able to bind the metal cations through the participation of two centers: the crown ether moiety and the heterocyclic part. The alkaline earth metal cations form complexes with the macrocyclic part of the molecule. The formation of a strong sandwich complex was found in the case of Ba^{2+}. The proton coordinates with the N atom of the heterocyclic fragment of the molecule. The Ag^+ and Hg^{2+} cations bind with both centers of the molecule: the crown ether fragment and the heterocyclic residue.

Introduction

The properties of the macrocyclic chromo- and fluoroionophores are being actively investigated in order to improve their characteristics which are useful in various fields: laser dyes, non-linear optics, potential sensitive dyes, biological probes, *etc.*[1a–f] Chromo- and fluoroionophores which play an important role in ion optical analysis are polymethine and styryl dyes.[2a–f] The complexing of a cation to the macrocyclic part of a dye leads to pronounced spectral shifts generating a change in signal which can be exploited for ion sensing.[3a–e] These compounds are able to selectively bind with metal cations, as demonstrated by the substantial changes occurring in optical properties upon complex formation. It was found that upon *trans–cis* isomerization the stability constant of the compounds could be changed by up to three orders of magnitude.

In the present paper the stability and the structure of complexes of the 2-styrylbenzothiazole containing 15-crown-5 ether moiety (**1**) with alkaline earth metal cations, proton, Ag^+, and Hg^{2+} were studied. This compound was chosen because it can bind alkaline earth metal cations by the crown ether fragment and could be a host for the heavy metal cations and proton due to the presence of the heterocyclic part. 2-Styrylbenzothiazoles containing azacrown ether fragments have been mentioned in the literature[2a–c] as fluorescent sensors for alkaline earth metal cations. We are interested in preparing and studying this ditopic receptor whose two binding places indicate substantial differences in optical response upon complex formation with metal cations of various types.

Results and discussion

Synthesis of the crown-containing 2-styrylbenzothiazole

We devised different methods to prepare 2-styrylbenzothiazole **1** containing a 15-crown-5 ether fragment (Scheme 1).

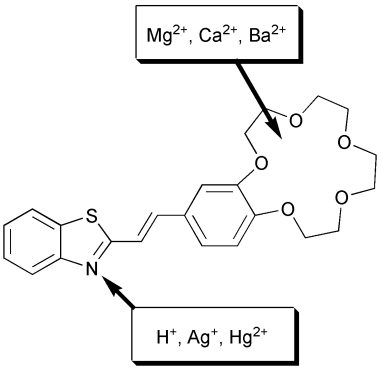

2-Methylbenzothiazole **2** and phosphonium salt **3**[4] were condensed with formyl derivatives of benzo-15-crown-5 ether **4**[5] in the presence of an equimolar amount of NaOMe in DMSO at ambient temperature for 24 h to form **1** with 53% and 63% yields (*Methods A*, *B*, Scheme 1). Heating reactants **2** and **4** with concentrated HCl at 100–130 °C for 3 h results in compound **1** in 23% yield, and some resinification occurs in course of the process (*Method C*, Scheme 1). The dye **6**[6] was obtained by reaction of 2,3-dimethylbenzothiazolium iodide[7] with **4** in boiling ethanol containing Py as a catalyst. Dye **6** produces **1** in 47% yield upon heating with PPh_3 (*Method D*, Scheme 1). The condensation of malonic acid with **4** results in the formation of the known cinnamic acid containing crown-15-ether-5 fragment[8] which can react with *o*-aminophenol in benzene to form **1** in 16% yield (*Method E*, Scheme 1). Among the reactions under study, the one-step *method A* seems to be the most simple with a quite good yield for **1**. In contrast, the yield of **1** using methods *C* and *E* is low, whereas for methods *B*, *D* and *E* a multistep synthesis is needed.

Structural identification of **1** in solution was based on its ^{1}H-NMR spectra (see Experimental section). Assignment of *E* configuration to **1** was on the basis of the spin–spin coupling

 DOI: 10.1039/b205305e

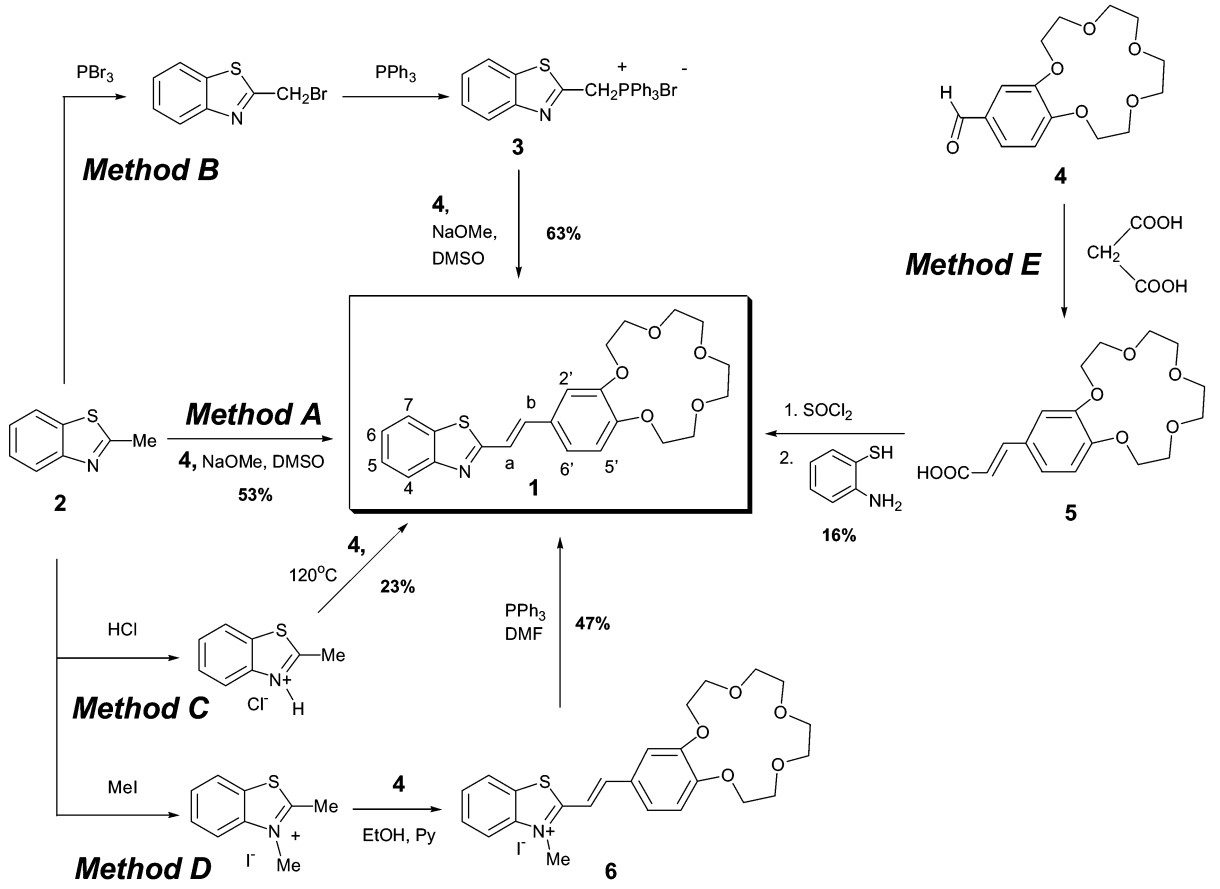

Scheme 1

constant for the olefinic protons, $^{3}J_{trans}$ = 15.6 Hz. For compound **1** the existence of four isomers **A**, **B**, **C**, **D** (Scheme 2) may be suggested. Isomers **A** and **B** possess *anti*-disposition of substituents near the ethylenic double bond, whereas in isomers **C** and **D** the substituents are in *syn*-disposition. An interaction between the ethylenic proton H(b) and the proton H(6′) in the benzene ring of the benzocrown ether can be observed in the NOESY spectrum only for isomer **A**, between proton H(b) and H(2′) for isomer **B**, an interaction between H(a) and the proton H(2′) can be found for isomer **C**, and between H(a) and H(6′) for isomer **D**. The obtained NOESY spectrum of compound **1** showed that all the interactions mentioned above between the ethylenic proton H(a) and H(b) and the protons H(2′) and H(6′) in the benzene ring of the benzocrown ether fragment take place indicating that compound **1** exists in MeCN solution as a mixture of the four isomers **A**, **B**, **C**, **D** (Scheme 2).

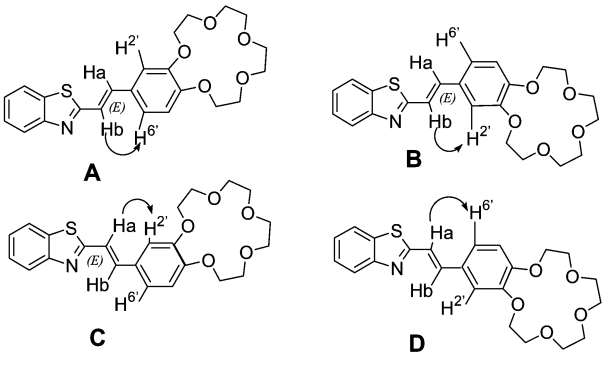

Scheme 2

Molecular geometry of 1

Front and side views and the atom labelling scheme for **1** are shown in Fig. 1. The central fragment of the molecule involving the thiazole ring and the ethylene bond is disordered over two positions. The disordered central fragment is depicted using full and open lines for the two positions. This disorder pattern indicates that the two (**A** and **B**) conformers of the compound are obtained in the crystal state. Because all atoms of the disordered fragment are located with low precision, there is no sense in discussing the geometry of this part of the molecule in detail. By contrast, geometric parameters of

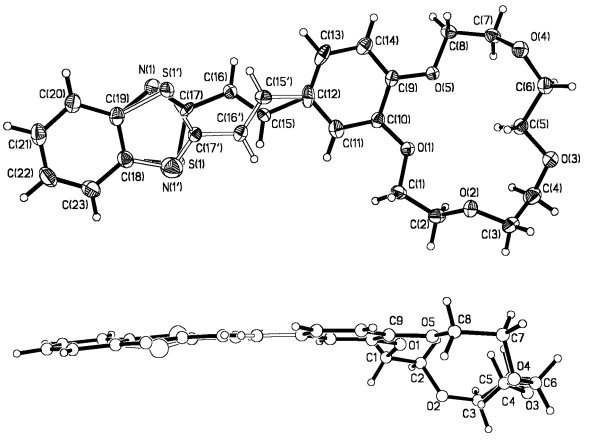

Fig. 1 Front (above) and side (below) projections of structure **1** with atom labelling scheme. Thermal ellipsoids are drawn at the 50% probability level. The disordered positions of the central part are depicted with full and open lines and the corresponding atoms for these disordered positions are denoted as numbers and primed numbers, respectively.

Table 1 Selected bond lengths [d/Å] and angles [ω/°] in **1**

Bond	d	Bond	Ų
O(1)–C(10)	1.376(3)	O(5)–C(9)	1.367(3)
O(1)–C(1)	1.442(3)	O(5)–C(8)	1.440(3)
O(2)–C(2)	1.427(3)	C(9)–C(10)	1.411(3)
O(2)–C(3)	1.430(3)	C(9)–C(14)	1.384(3)
O(3)–C(5)	1.424(3)	C(10)–C(11)	1.381(3)
O(3)–C(4)	1.430(3)	C(11)–C(12)	1.413(4)
O(4)–C(6)	1.434(3)	C(12)–C(13)	1.385(4)
O(4)–C(7)	1.434(3)	C(13)–C(14)	1.403(4)
Angle	ω	Angle	ω
C(10)–O(1)–C(1)	117.4(2)	O(5)–C(9)–C(14)	125.1(2)
C(2)–O(2)–C(3)	114.1(2)	O(5)–C(9)–C(10)	115.4(2)
C(5)–O(3)–C(4)	114.7(2)	O(1)–C(10)–C(11)	125.5(2)
C(6)–O(4)–C(7)	114.7(2)	O(1)–C(10)–C(9)	114.2(2)
C(9)–O(5)–C(8)	118.1(2)		

the benzocrown ether moiety and the benzothiazole benzene ring have been determined rather accurately. Selected bond lengths and angles are listed in Table 1. The molecule is near planar. A slight twist of the molecule about its long dimension is observed. The dihedral angle between the benzene rings is equal to 13.6°.

In general, the molecule exhibits geometric peculiarities (see Table 1) typical of all compounds involving the benzocrown ether moiety.

The geometric parameters at the O(1) and O(5) oxygen atoms indicate their sp^2 hybridization state, in contrast to those at the other oxygen atom corresponding to the sp^3 hybridization state. In fact, the bond angles at O(1) and O(5) are equal to 117.4° and 118.1°, whereas the bond angles at the other oxygen atoms vary within 114.1(2)–114.7(2)°. Torsion angles C(1)–O(1)–C(10)–C(11) (−13.9°) and C(8)–O(5)–C(9)–C(14) (−0.9°) are close to the ideal value for conjugation of the lone pair of each of the O(1) and O(5) atoms occupying the p orbital with the benzene ring. In spite of a rather close contact between the O(1) and O(5) atoms (2.56 Å), the endocyclic angles O(1)–C(10)–C(9) and O(5)–C(9)–C(10) are reduced (114.2(2)° and 115.4(2)°), whereas the exocyclic angles O(1)–C(10)–C(11) and O(5)–C(9)–C(14) are increased (125.5(2) and 125.1(2)°, respectively).

One more specific feature of structure **1** is an alternation of the C–C bond in the C(9)···C(14) benzene ring. The C(9)–C(10), C(11)–C(12) and C(13)–C(14) bonds [1.411(3), 1.413(4), and 1.403(4) Å] are longer than the C(10)–C(11), C(12)–C(13), and C(9)–C(14) bonds [1.381(3), 1.385(4), and 1.384(3) Å, respectively]. This alternation together with the aforementioned angular distortion may be rationalized by assuming a conjugation phenomenon; the lone electron pair located on the p orbital of each of O(1) and O(5) atoms would be involved in this conjugation.

The conformation of the crown ether is irregular, which is clearly seen from Fig. 1. The O(3) and O(4) atoms are oriented outside of the macrocycle.

The lack of stacking is the most interesting peculiarity of the crystal packing of compound **1**. Fig. 2 shows two projections of the crystal packing of **1**.

The dye molecules are arranged in staircases rather than stacks:

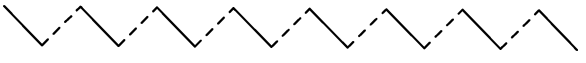

Adjacent molecules in a staircase are related by a translation. Such a structural motif may be considered as originating from a stack with the "head-to-head" mutual arrangement at the cost of a glide of each molecule in all adjacent pairs of molecules in opposite directions. These staircases form layers. Also the crown ether moieties form double layers. Both types of layers alternate in the crystal.

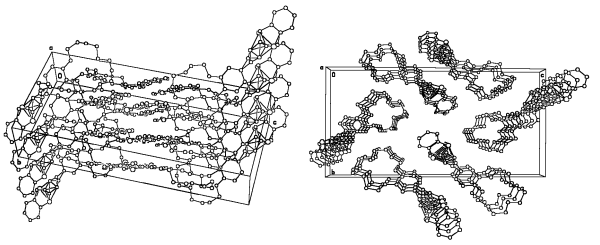

Fig. 2 Two projections of crystal packing of **1**. The dye moieties of molecules are arranged in staircases rather than stacks to form layers. The crown ether moieties also form layers. The two types of layers alternate in the crystal.

Complex formation of 1 with alkaline earth metal cations, $HClO_4$ and $Hg(ClO_4)_2$

The *E*-isomers of **1** exhibit strong absorption and fluorescence emission in the visible region, as shown in Fig. 3. The addition of alkaline earth metal (Mg, Ca, Ba) perchlorates to a solution of **1** in MeCN resulted in hypsochromic shifts of the long wavelength absorption band and of the fluorescence band, which are evidently due to formation of complexes of the alkaline earth metal cations with the crown ether fragment of the molecule (Scheme 3). The fluorescence quantum yield of **1** increased upon complex formation (Fig. 3, Table 2).

The equilibrium constants for complex formation of **1** with Mg^{2+} Ca^{2+}, Ba^{2+}, H^+ and Hg^{2+} were calculated from the absorption spectra of solutions at constant ligand concentration and varying metal perchlorate concentrations using the HYPERQUAD program,[9] designed for use in connection with studies of chemical equilibria in solution from data obtained on potentiometric and/or spectrophotometric titrations. The program uses a least-squares approach.

Three equilibria were studied:

$$L + M \overset{K_{11}}{\rightleftharpoons} LM \qquad K_{11} = \frac{[LM]}{[L]\cdot[M]}$$

$$L + 2M \overset{K_{12}}{\rightleftharpoons} LM_2 \qquad K_{12} = \frac{[LM_2]}{[L]\cdot[M]^2}$$

$$2L + M \overset{K_{21}}{\rightleftharpoons} L_2M \qquad K_{21} = \frac{[L_2M]}{[L]^2\cdot[M]}$$

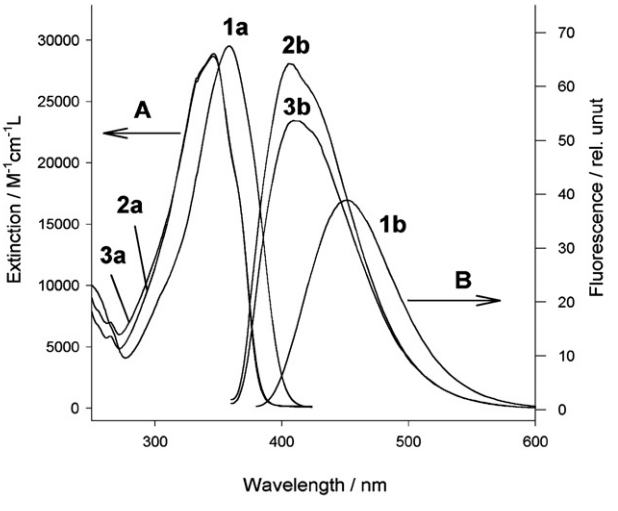

Fig. 3 Absorption (A) and fluorescence (B) spectra of dye **1** as free ligand (1a,b) and as complexes with Mg^{2+} (2a,b) and Ca^{2+} (3a,b). All spectra were recorded in acetonitrile at [**1**] = 2.9×10^{-5} M, [Mg^{2+}] = 4×10^{-4} M, [Ca^{2+}] = 4×10^{-4} M.

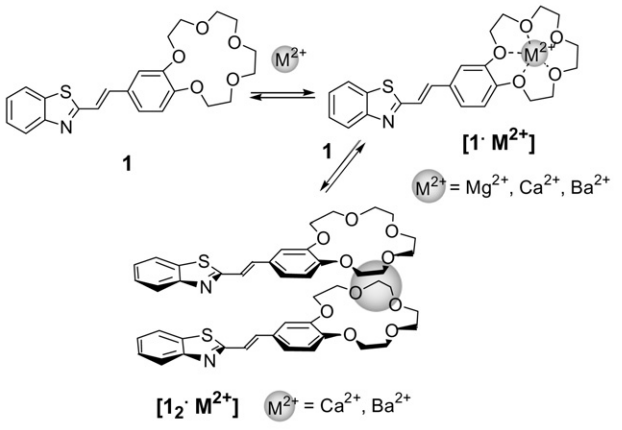

Scheme 3

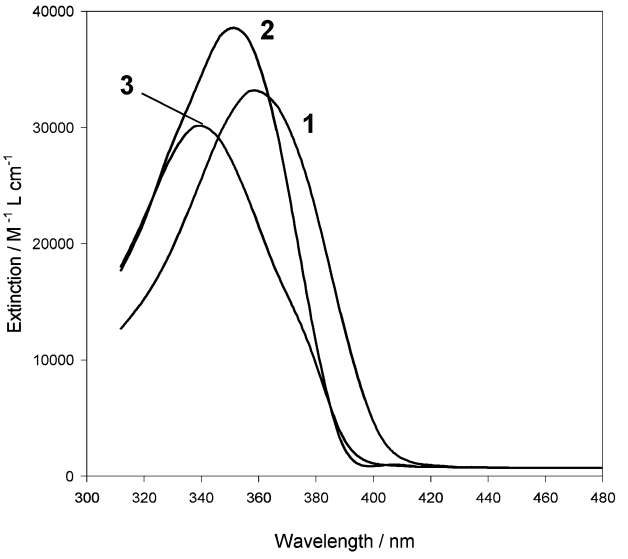

Fig. 4 Absorption spectra of dye **1** as free ligand (1) and its complexes [**1**·Ba^{2+}] (2) and [$\mathbf{1}_2$·Ba^{2+}] (3) calculated from spectrophotometric titration data using the Hyperquad program. Values of extinction coefficient for complex [$\mathbf{1}_2$·Ba^{2+}] are reduced twice for convenience of representation.

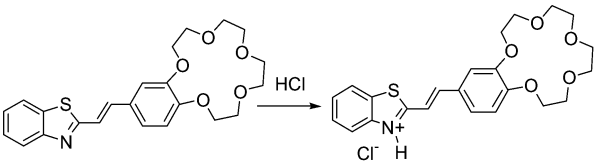

Scheme 4

It was found that ligand **1** formed one kind of complex with Mg^{2+}, namely [**1**·Mg^{2+}] (Table 2). A distinct isosbestic point upon spectrophotometric titration of **1** with Mg^{2+} was observed, confirming only one kind of complex formation. For Ca^{2+} and Ba^{2+} the distortion of an isosbestic point was observed upon spectrophotometric titration, indicating more than one kind of complex formation. Two kinds of complexes were found for Ca^{2+} and Ba^{2+}, [**1**·M^{2+}] and [$\mathbf{1}_2$·M^{2+}] (M = Ca^{2+}, Ba^{2+}), by treatment of spectrophotometric titration data using the HYPERQUAD program. In the case of Ba^{2+} the sandwich complex formed possesses the highest stability. Fig. 4 shows that the spectra of [**1**·Ba^{2+}] and [$\mathbf{1}_2$·Ba^{2+}] complexes calculated from spectrophotometric titration data differ from each other. According to the NMR study of the sandwich complex [$\mathbf{1}_2$·Ba^{2+}], molecules of the dye are arranged in a "head-to-head" stacking fashion in this complex (Scheme 3). This conclusion is based on the upfield shifts of the aromatic proton signals in the sandwich complex in comparison with those in the free ligand (see Experimental section). The changes in NMR could be due to ring-current effects produced by the adjacent conjugated molecules.

Addition of $HClO_4$ to an acetonitrile solution of **1** resulted into the formation of a perchlorate salt of **1** whose the long wavelength absorption band was red shifted relative to the corresponding free ligand **1** (Scheme 4, Fig. 5).

Addition of Hg perchlorate to the acetonitrile solution of the dye **1** produced also a red-shift of the UV spectrum relative to the free ligand similarly to that observed in the case of the proton addition. The results of the spectrophotometric titration reveal the formation of two complexes. At first, upon the addition of $Hg(ClO_4)_2$ to the dye solution the bathochromic shift occurs, indicating the formation of complex [**1**·Hg^{2+}] through the heterocyclic part of the molecule (Scheme 5). At higher Hg^{2+} concentration the formation of [**1**·$(Hg^{2+})_2$] is observed; its stability constant is indicated in Table 2. The formation of the [**1**·$(Hg^{2+})_2$] complex is accompanied by a blue shift of a long wavelength absorption band which means that the second Hg^{2+} ion is bound to the crown ether moiety (Scheme 5, Fig. 6).

Finally, we prepared the mixed complex of [$\mathbf{1}_2$·Ba^{2+}] with Hg^{2+} by adding $Hg(ClO_4)_2$ to the acetonitrile solution of [$\mathbf{1}_2$·Ba^{2+}]. The long wavelength absorption band of the mixed complex was found to be blue shifted relative to the [**1**·Hg^{2+}] spectrum and red shifted relative to the [$\mathbf{1}_2$·Ba^{2+}] absorption band (Fig. 7). Due to the complexity of the system we did not determine the stoichiometry and stability constant for the mixed complex.

The hypsochromic or bathochromic shifts observed upon complex formation in crown-containing stilbene-like molecules can be explained by changes in electronic interactions, as discussed in detail in some previous publications.[10a–e] When a chromophore contains an electron-donating group conjugated to an electron-withdrawing group, it undergoes intramolecular charge transfer from the donor to the acceptor upon excitation

Table 2 Steady-state absorption, fluorescence data and stability constants for **1** and its complexes with Mg^{2+}, Ca^{2+}, Ba^{2+}, H^+ and Hg^{2+} in acetonitrile at 20 °C

	1	**1**·Mg^{2+}	**1**·Ca^{2+}	**1**·Ba^{2+}	**1**·H^+	**1**·Hg^{2+}
λ^{abs}_{max}/nm	358	346	346	350	426	423
$\varepsilon \times 10^{-4}$/$M^{-1}$ cm^{-1} L	3.3	3.23	3.23	3.8[a]	3.5	3.15[a]
λ^{fl}_{max}/nm[d]	452	406	410	446[b]	545	523[c]
φ^{fl}	0.0135	0.020	0.018	0.037[b]	0.021	0.037[c]
Log K_{11}		5.5 ± 0.1	5.6 ± 0.1	4.7 ± 0.1	6.4 ± 0.5	5.6 ± 0.1
Log K_{21}			10.3 ± 0.2	10.8 ± 0.2		
Log K_{12}						9.4 ± 0.15

[a] Calculated using the Hyperquad program.[9] [b] For complex $(\mathbf{1})_2$·Ba^{2+}. [c] For complex **1**·$(Hg^{2+})_2$. [d] Exitation at 347 nm.

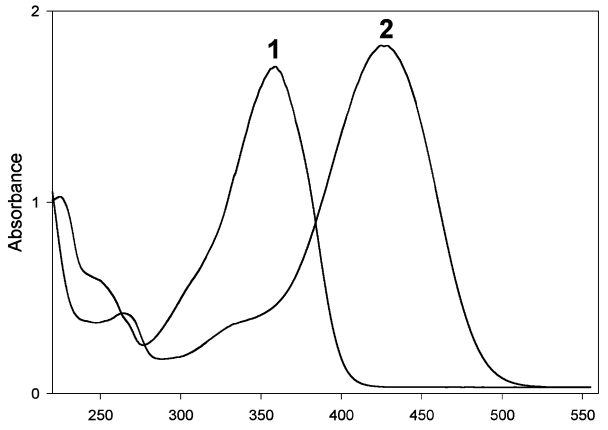

Fig. 5 Absorption spectra of dye **1** as the free ligand (1) and as complex [**1**·H$^+$] (2) in acetonitrile at 20 °C. Concentrations of **1** and [**1**·H$^+$] are both 5×10^{-5} M.

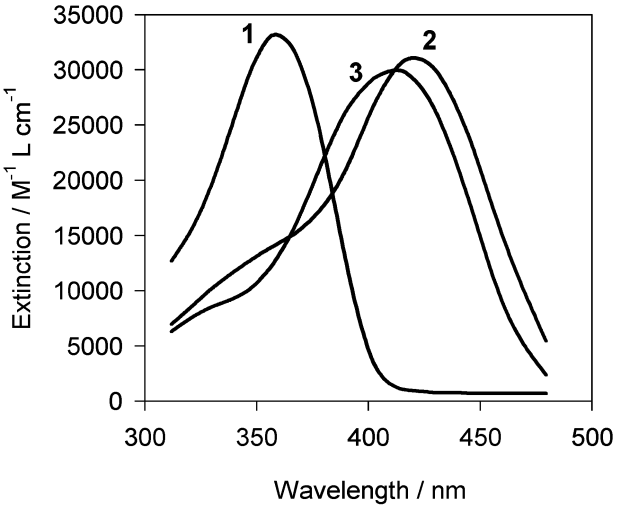

Fig. 6 Absorption spectra of dye **1** as free ligand (1) and as complexes [**1**·Hg^{2+}] (2) and [**1**·(Hg^{2+})$_2$] (3) calculated from spectrophotometric titration data using the Hyperquad program.

by light. It can thus be postulated that cations in close interaction with the electron-donor or acceptor moiety will affect the efficiency of the intramolecular charge transfer. Therefore when a group playing an electron-donor role interacts with a cation, the latter should reduce the electron-donating character of the group, resulting into a decrease of the conjugation. As a consequence, it can be expected that a blue shift of the absorption spectrum takes place together with a decrease of the extinction coefficient. Conversely, a cation interacting with an electron-acceptor group should enhance the electron-withdrawing character of the group, producing a red-shift of the absorption spectrum.

Molecular geometry and crystal packing of complex [1 · (Ag$^+$)$_2$]

Addition of $AgNO_3$ to the dye **1** solution provokes too small changes in UV spectrum to allow the measurement of the stability constant or to determine the stoichiometry of the complex. But we were able to find the experimental conditions needed to prepare an Ag complex of dye **1**, with a 2:1 stoichiometry [**1**·(Ag$^+$)$_2$] demonstrated by a crystallographic study (see Experimental part). Front and side views and the atom labelling scheme for [**1**·(Ag$^+$)$_2$] are shown in Fig. 8. Only the *syn* isomer of the dye occurs in the crystal of the complex. The Ag cations are coordinated to both coordination positions of the dye, including the crown ether and the benzothiazole moieties.

The geometric parameters of the dye molecule in the 2:1 complex are close to those found for **1**. Selected bond lengths and angles are listed in Table 3. The molecule is near planar with the dihedral angle between two benzene rings being equal to 7.2°. The C(14)–C(9)–C(10)–C(11)–C(12) benzene ring fragment of the benzocrown ether exhibits a distinct bond alternation (1.381(8), 1.413(7), 1.374(7), and 1.419(7) Å, respectively), whereas the C(14)–C(13)–C(12) fragment shows almost complete bond delocalisation (1.392(8), and 1.398(8) Å). This peculiarity may be due to a weak coordination of the C(12)–C(13)–C(14) fragment to the Ag(1) atom of the adjacent formula unit in the crystal packing (see below).

The geometry of the crown ether O(1) and O(5) oxygen atoms agrees well with that found for **1**, which indicates the conjugation of these oxygen atoms with the benzene ring. For instance, the angles at these oxygen atoms [117.4°(4) and 118.3°(4)] correspond to the sp^2 hybridisation state, whereas the angles at the other oxygen atoms [111.5°(4)–114.4°(4)] correspond to the sp^3 hybridisation state. The C(1)–O(1)C(10)–C(11) and C(8)–O(5)–C(9)–C(14) torsion angles C–O–C$_{(Ar)}$–C$_{(Ar)}$ are equal to 8.3° and −9.2°, respectively.

The clearly alternating bond lengths in the ethylene fragment [C(12)–C(15) 1.458(7), C(15)–C(16) 1.335(8), and

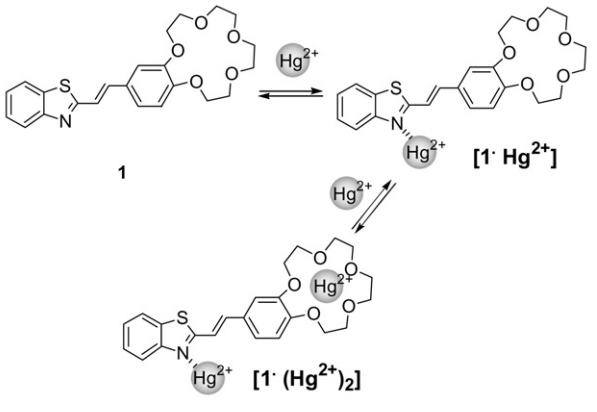

Scheme 5

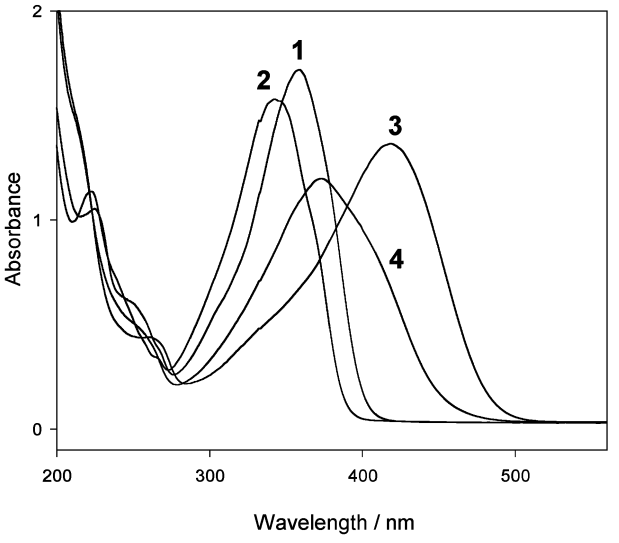

Fig. 7 Absorption spectra of dye **1** as free ligand (1) and as complexes [**1**$_2$·Ba^{2+}] (2), [**1**·Hg^{2+}] (3) and [**1**$_2$·Ba^{2+},Hg^{2+}] (4) in acetonitrile at 20 °C. (1) [**1**] = 5×10^{-5} M; (2) [**1**$_2$·Ba^{2+}] = 2.5×10^{-5} M; (3) [**1**·Hg^{2+}] = 5×10^{-5} M; (4) [**1**$_2$·Ba^{2+}] = 2.5×10^{-5} M and [Hg^{2+}] = 1×10^{-4} M.

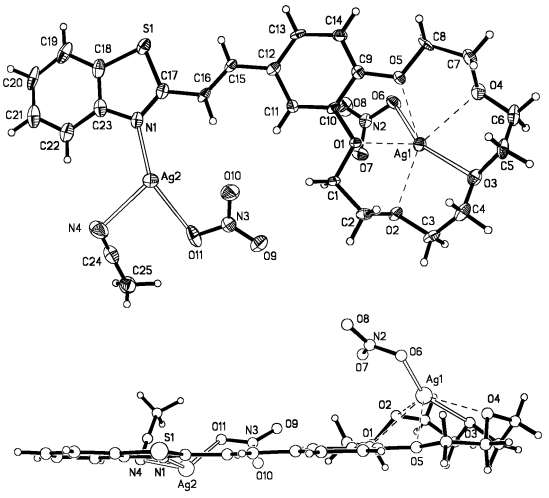

Fig. 8 Front (above) and side (below) projections of the structure of [**1**·$(Ag^+)_2$] with atom labelling scheme. Thermal ellipsoids are drawn at the 50% probability level.

C(16)–C(17), 1.452(7) Å] indicate that the conjugation within this fragment is reduced.

A coordination pattern of both silver atoms [Ag(1) and Ag(2)] is presented in Fig. 9, showing a fragment of the crystal packing. Selected parameters of the coordination environments of both silver atoms are given in Table 4. The Ag(1) atom is coordinated with the five crown ether oxygen atoms [Ag(1)···O bond lengths varying in the range 2.426(4)–2.721(4) Å] and the O(6) oxygen atom [2.367(4) Å] of the nitrate group. An irregular bidentate type coordination of the nitrate group could be considered too [the Ag···O(7) distance is equal to 2.661(4) Å]. The interaction of $Ag(NO_3)$ moiety with 18-crown-6 was investigated previously in our theoretical work.[11] The results of this X-ray diffraction experiment completely confirm our theoretical predictions based on DFT calculations:[11] the Ag^+ ion is coordinated to crown ether oxygen atoms and to the bidentate nitrate group. According to our theoretical predictions, the Ag^+ ion is displaced out of the (average) plane of crown ether oxygen atoms. The coordination of the Ag(1) is irregular. The coordination polyhedron may be approximately described as a pentagonal prism with

Table 3 Selected bond lengths [d/Å] and angles [ω/°] in the crown ether dye moiety in [**1**·$(Ag^+)_2$]

Bond	d	Bond	d
O(1)–C(10)	1.362(6)	C(11)–C(12)	1.419(7)
O(1)–C(1)	1.439(6)	C(12)–C(13)	1.398(8)
O(2)–C(2)	1.430(6)	C(13)–C(14)	1.392(8)
O(2)–C(3)	1.426(6)	C(14)–C(9)	1.381(8)
O(3)–C(4)	1.438(7)	C(12)–C(15)	1.458(7)
O(3)–C(5)	1.448(7)	C(15)–C(16)	1.335(8)
O(4)–C(6)	1.441(7)	C(16)–C(17)	1.452(7)
O(4)–C(7)	1.426(7)	C(17)–S(1)	1.767(6)
O(5)–C(8)	1.433(6)	S(1)–C(18)	1.732(6)
O(5)–C(9)	1.366(6)	C(17)–N(1)	1.304(7)
C(9)–C(10)	1.413(7)	N(1)–C(23)	1.401(7)
C(10)–C(11)	1.374(7)		
Angle	ω	**Angle**	ω
C(10)–O(1)–C(1)	117.4(4)	O(1)–C(10)–C(11)	125.2(5)
C(2)–O(2)–C(3)	114.4(4)	O(1)–C(10)–C(9)	113.8(4)
C(4)–O(3)–C(5)	111.5(4)	O(5)–C(9)–C(14)	124.6(5)
C(6)–O(4)–C(7)	113.0(5)	O(5)–C(9)–C(10)	115.7(5)
C(8)–O(5)–C(9)	118.3(4)		

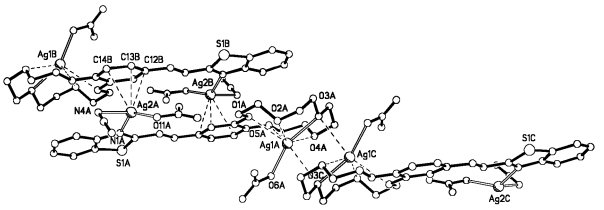

Fig. 9 Fragment of crystal packing of [**1**·$(Ag^+)_2$] showing full coordination environment of the metal atoms [Ag(1A) and Ag(2A); a letter in the atom labels shows that the atoms belong to different formula units in the crystal packing]. The formula units in the pairs A–B and A–C are related by symmetry centres belonging to different systems.

the O(6) atom in the apical position. However, an original linear coordination O(3)–Ag(1)–O(6) [155.4(1)°] is obviously visible, distorted by other, weaker Ag(1)···O interactions. The oxygen atoms of the crown ether moiety are arranged as an almost regular pentagon. The O···Ag(1)···O angles vary within 56.4(1)–77.6(1)°. The average C–O–Ag(1) angles at each of the oxygen atoms vary within 109.9(3)–114.4(3)°, which indicates that one of the lone electron pairs of the O(2), O(3), and O(4) atoms is pointing toward the Ag(1) atom. However, in the case of the O(1) and O(5) atoms having the sp^2 hybridization state, the corresponding angles are less favorable for the coordination of these atoms with Ag(1). As a result the distances between Ag(1) and these oxygen atoms are the longest ones.

The Ag(2) atom has a distorted trigonal planar geometry. It binds to the N(1) atom of the benzothiazole moiety and it is coordinated by one oxygen [O(11)] atom of the second nitrate group and the N(4) atom of a solvated acetonitrile molecule. The Ag(2)···N(1), Ag(2)–O(11), and Ag(2)–N(4) distances are 2.236(5), 2.406(5), and 2.462(5) Å and the angles at Ag(2) vary within 138.8(2)–81.6(2)°. According to ref. 12, irregular or distorted coordination polyhedra are typical for compounds of Ag(I) and Au(I).

In a crystal of [**1**·$(Ag^+)_2$], both silver atoms participate additionally in weak interactions (see Fig. 9). The Ag(1) atom forms a secondary bond with the O(3) atom of an adjacent molecule in the crystal. The corresponding distance is equal

Table 4 Geometry of coordination environment of Ag atoms in [**1**·$(Ag^+)_2$]

Distance	d	Distance	d
Ag(1)–O(1)	2.690(4)	Ag(2)–O(11)	2.406(5)
Ag(1)–O(2)	2.607(4)	Ag(2)–N(1)	2.236(5)
Ag(1)–O(3)	2.426(4)	Ag(2)–N(4)	2.462(5)
Ag(1)–O(4)	2.659(4)	Ag(2)–C(12^b)	3.185(6)
Ag(1)–O(5)	2.721(4)	Ag(2)–C(13^b)	2.750(6)
Ag(1)–O(6)	2.367(4)	Ag(2)–C(14^b)	2.929(6)
Ag(1)–O(3^a)	3.061(4)		
Angle	ω	**Angle**	ω
O(6)–Ag(1)–O(5)	77.6(1)	O(3)–Ag(1)–O(4)	69.1(1)
O(1)–Ag(1)–O(2)	63.4(1)	O(4)–Ag(1)–O(5)	62.2(1)
O(2)–Ag(1)–O(3)	69.3(1)	O(1)–Ag(1)–O(5)	56.4(1)
O(3)–Ag(1)–O(6)	155.4(1)	C(2)–O(2)–Ag(1)	116.7(3)
O(11)–Ag(2)–N(1)	138.8(2)	C(4)–O(3)–Ag(1)	115.0(3)
O(11)–Ag(2)–N(4)	81.6(2)	C(5)–O(3)–Ag(1)	113.8(3)
N(1)–Ag(2)–N(4)	111.3(2)	C(7)–O(4)–Ag(1)	117.6(3)
C(10)–O(1)–Ag(1)	109.8(3)	C(6)–O(4)–Ag(1)	105.6(3)
C(1)–O(1)–Ag(1)	110.0(3)	C(9)–O(5)–Ag(1)	108.7(3)
C(3)–O(2)–Ag(1)	106.1(3)	C(8)–O(5)–Ag(1)	111.2(3)

Symmetry transformations used to generate equivalent atoms: ^{a} $-x$, $-y+2$, $-z+1$; ^{b} $-x$, $-y+1$, $-z$.

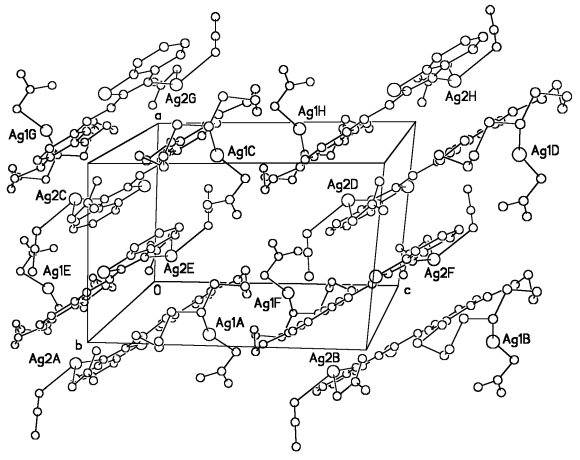

Fig. 10 General view of crystal packing of [**1**·$(Ag^+)_2$]. Only Ag atoms are denoted; a letter in the atom labels shows the Ag atoms belong to different formula units in the crystal packing. The formula units A–E–C–G and B–F–D–H form two stacks.

to 3.061(4) Å. The Ag(2) atom is weakly coordinated by the C(12)–C(13)–C(14) fragment of the other adjacent molecule. The distances Ag(2)···C(12), Ag(2)···C(13), and Ag(2)···C(14) are equal to 3.185(6), 2.750(6), and 2.929(6) Å. These weak interactions play an important role in governing the particular supramolecular architecture of the complexed dye molecules. Within this architecture, only the *syn* isomer (**A**) of the crown ether dye molecule is allowed to exist, although crystals of the starting compound **1** contain two isomers (**A** and **B**). It is obvious that the *anti* isomer (**B**) could not be cocrystallised with the *syn* isomer within the available organization of the molecules. Hence, we may conclude that crystallization of complexes can be used for separation of the pure *anti*-isomer.

The dye molecules are arranged in stacks in the crystal packing of [**1**·$(Ag^+)_2$] (see Fig. 10). Each molecule in a stack is related to both adjacent molecules through symmetry centres, which corresponds to a "head-to-tail" mutual arrangement. The stacks are arranged in layers. In the crystal, the layers of stacks alternate with layers formed by crown ether moieties.

Conclusion

Thus, in this paper using UV-visible absorption and fluorescence spectrophotometric and X-ray diffraction data, we have demonstrated the possibility of studying the binding of receptor **1** to various metal cations through the participation of two centers in the dye molecule, including the crown ether moiety and the heterocyclic part. Both centers possess different selectivities to the metal cations, although the optical response to the complexation process differs at both binding sites. This investigation can be considered as an important step in the development of novel selective optical sensors for metal cations.

Experimental

Materials

2-Methylbenzothiazole (**2**), triphenylphosphine, phosphorus tribromide, 2-aminothiophenol, malonic acid were commercially available. 2,3,5,6,8,9,11,12-Octahydro-1,4,7,10,13-benzopentaoxacyclopentadecine-15-carbaldehyde[5] (**4**), (*E*)-3-(2,3,5,6,8,9,11,12-octahydro-1,4,7,10,13-benzopentaoxacyclopentadecin-15-yl)-2-propenoic acid[8] (**6**), (1,3-benzothiazol-2-ylmethyl)-(triphenyl)phosphonium bromide[4] (**3**), 3-methyl-1,3-benzothiazol-3-ium iodide[7] were synthesized according to known procedures.

Anhydrous $Mg(ClO_4)_2$ (Aldrich) was used as received. Spectroscopic grade acetonitrile was distilled over CaH_2 to remove traces of water. Solutions of dye **1** were prepared and used under red light.

Synthesis and characterization

^{1}H NMR spectra were recorded on Bruker AMX-400 and Bruker DRX-500 spectrometers using TMS as the internal standard and CD_3CN as the solvent. The chemical shifts and the spin–spin coupling constants were determined with an accuracy of 0.01 ppm and 0.1 Hz, respectively. Mass spectra were obtained using a Varian MAT 311A instrument with an ionisation energy of 70 eV. The preparation reactions were monitored by TLC on DC-Alufolien Kieselgel 60 F_{254} (Merck) and DC-Alufolien aluminium oxide 60 F_{254} neutral (Type E) plates. For column chromatography, aluminium oxide 150 basic (Type T) was used.

NaOMe was prepared by the solution of Na in anhydrous MeOH, evaporation of the excess of MeOH, and drying of the salt under vacuum.

Method A. A mixture of **2** (1 mmol), **4** (1.1 mmol) and NaOMe (1 mmol) in 20 ml of anhydrous DMS was kept at ambient temperature for 24 h. After adding distilled water, the product was extracted into benzene and purified by column chromatography on aluminium oxide (eluent: benzene–EtOH, 40:1) followed by crystallization from MeOH to afford **1** in 53% yield, m.p. 139–140 °C, ^{1}H NMR (500 MHz, $CDCl_3$) δ 3.95 (d, 6H, $2OCH_3$), 6.91 (d, 1H, H-5′, $J = 8.0$), 7.16 (m, 2H, H-6′, H-2′), 7.31 (d, 1H, H-a, $J = 16.1$), 7.37 and 7.48 (2 m, 2H, H-5, H-6), 7.48 (d, 1H, H-b, $J = 16.2$), 7.87 and 7.99 (2 d, 2H, H-4, H-7, $J = 7.9$, $J = 8.0$); m/z ($I_{rel.}$, %): 297 (69) [M^+], 296 (96), 282 (17), 239 (22), 223 (16), 210 (24), 149 (17), 105 (26), 77 (16), 63 (22), 58 (47). Anal. calcd for $C_{17}H_{15}NO_2S$: C 68.66, H 5.08, N 4.71. Found: C 68.46, H 5.01, N 4.71%.

Method B. A solution of **3** (1.1 mmol) in 10 ml of anhydrous DMSO was dropwise added to a mixture of **4** (1 mmol) and NaOMe (1 mmol) in 20 ml of anhydrous DMSO at 0 °C. The resulting mixture was stirred for 1 h at 0 °C, and for 3 h at ambient temperature. Then the mixture was kept for 24 h at ambient temperature. After addition of distilled water, the product was extracted into benzene and purified by column chromatography on aluminium oxide (eluent: benzene–EtOH, 40:1) followed by crystallization from MeOH to afford **1** in 63% yield.

Method C. A mixture of **2** (1 mmol) and conc. HCl (1.2 mmol) was heated for 0.5 h at 80 °C. The excess of HCl was evaporated, and the residue of hydrochloride of **2** was crystallized from EtOH. The mixture of hydrochloride of **2** (1 mmol) and **4** (1 mmol) was heated for 8 h at 120 °C. The obtained residue was dissolved in an aqueous solution of Na_2CO_3 and the product was extracted into benzene. After evaporation of the solvent, the product was purified by column chromatography on aluminium oxide (eluent: benzene–EtOH, 40:1) to afford **1** in 23% yield.

Method D. 3-Methyl-2-[(*E*)-2-(2,3,5,6,8,9,11,12-octahydro-1,4,7,10,13-benzopentaoxacyclopentadecin-15-yl)-1-ethenyl]-1,3-benzothiazol-3-ium iodide (**6**) was synthesized according to a known procedure[6] with 79% yield, m.p. 143–146 °C, ^{1}H NMR (500 MHz, DMSO-d_6) δ 3.95 (d, 6H, $2OCH_3$), 6.91 (d, 1H, H-5′, $J = 8.0$), 7.16 (m, 2H, H-6′, H-2′), 7.31 (d, 1H, H-a, $J = 16.1$), 7.37 and 7.48 (2 m, 2H, H-5, H-6), 7.48 (d, 1H, H-b, $J = 16.2$), 7.87 and 7.99 (2 d, 2H, H-4, H-7, $J = 7.9$, $J = 8.0$). Anal. calcd for $C_{24}H_{28}NO_5SI \times 0.5\ H_2O$: C 49.83, H 5.05, N 2.42. Found: C 49.76, H 4.98, N 2.27%.

A solution of 0.1 g (0.3 mmol) **6** and 0.94 g (0.36 mmol) PPh_3 in 20 ml DMF was boiled for 10 h, followed by removal of solvent. The residue was dissolved in an aqueous solution of HCl, unreacted compounds were extracted by benzene. The aqueous solution of Na_2CO_3 was added to the acidic solution and the product was extracted into benzene. After evaporation of the solvent, the product was purified by column chromatography on aluminium oxide (eluent: benzene–EtOH, 40:1) to afford **1** in 47% yield.

Method E. 0.2 ml (1.5 mmol) of $SOCl_2$ was added dropwise to a solution of 0.1 g (0.3 mmol) **5** in 2 ml of anhydrous benzene for 0.5 h. The mixture was heated for 1 h at 60 °C, followed by removing of solution and excess of $SOCl_2$. The residue was dissolved in 5 ml of anhydrous benzene. The resulting solution was added dropwise to a solution of 0.037 g (0.3 mmol) *o*-aminophenol in 2 ml of anhydrous benzene for 0.5 h. The mixture was boiled for 2 h and filtered. The solvent was removed in *vacuum*, the product **1** was crystallized from MeOH (16% yield).

Synthesis of the complex of (*E*)-1 with $Ba(ClO_4)_2$. $Ba(ClO_4)_2$ (2.4 mg, 0.007 mmol) and (*E*)-**1** (6.0 mg, 0.014 mmol) were dissolved in 6 ml CD_3CN under red light. The resulting $[(E)\text{-}\mathbf{1}]_2{\cdot}Ba^{2+}$ was used for NMR investigation (500 MHz, CD_3CN) δ 3.95 (d, 6H, $2OCH_3$), 6.91 (d, 1H, H-5′, $J = 8.0$), 7.16 (m, 2H, H-6′, H-2′), 7.31 (d, 1H, H-a, $J = 16.1$), 7.37 and 7.48 (2 m, 2H, H-5, H-6), 7.48 (d, 1H, H-b, $J = 16.2$), 7.87 and 7.99 (2 d, 2H, H-4, H-7, $J = 7.9$, $J = 8.0$).

Synthesis of the complex of (*E*)-1 with $AgClO_4$. $AgClO_4$ (2.9 mg, 0.014 mmol) and (*E*)-**1** (6.0 mg, 0.014 mmol) were dissolved in 6 ml CH_3CN under red light. The resulting solution was used for growing crystals.

Spectroscopic measurements

UV-Vis spectra were recorded with a Specord-M40 spectrophotometer. Preparation of solutions and all measurements were carried out under red light. Steady-state fluorescence spectra were recorded on a Shimadzu RF-5000 spectrofluorometer. The fluorescence quantum yields of ligand and complex in air-saturated acetonitrile were determined at 20 ± 1 °C relative to fluorescein in 0.01 M NaOH in water ($\varphi_f = 0.92$)[13] with excitation at 365 nm. Quantum yields were based on integrated uncorrected fluorescence spectra.

Equilibrium constant determination. Complex formation of **1** with $Mg(ClO_4)_2$, $Ca(ClO_4)_2$, $Ba(ClO_4)_2$, $Hg(ClO_4)_2$ or $HClO_4$ in acetonitrile at 20 ± 1 °C was studied by spectrophotometric titration. The ratio of **1** to $Mg(ClO_4)_2$, $Ca(ClO_4)_2$, $Ba(ClO_4)_2$, $Hg(ClO_4)_2$ or $HClO_4$ was varied by adding aliquots of a solution containing known concentrations of **1** and of the corresponding salt or acid to a solution of **1** alone of the same concentration. The absorption spectrum of each solution was recorded and the stability constants of the complexes were determined using the Hyperquad program.[9] Ionic strengths varied from 0 to 8×10^{-4} M in the course of these titrations.

X-Ray crystallographic study

Crystallographic data and structure solution and refinement parameters for **1** and $[\mathbf{1}{\cdot}(Ag^+)_2]$ are given in Table 5. In both cases, a single crystal suitable for an X-ray diffraction experiment was coated with perfluorated oil and mounted on a

Table 5 Crystal data, data collection, structure solution and refinement parameters for **1** and its complex $[\mathbf{1}{\cdot}(Ag^+)_2{\cdot}CH_3CN]$

Compound	**1**	$[\mathbf{1}{\cdot}(Ag^+)_2{\cdot}CH_3CN]$
Empirical formula	$C_{23}H_{25}NO_5S$	$C_{25}H_{28}Ag_2N_4O_{11}S$
Formula weight	427.50	808.31
Colour, habit	yellow, plate	
Crystal size/mm	$0.26 \times \geqslant 0.18 \times 0.08$	$0.24 \times 0.14 \times 0.08$
Crystal system	Monoclinic	Triclinic
Space group	$P2_1/c$	$P\bar{1}$
Unit cell dimensions:		
a/Å	5.0566(7)	9.4310(5)
b/Å	14.156(2)	11.6540(6)
c/Å	28.558(4)	13.4464(7)
α/°	90.0	88.270(3)
β/°	93.492(8)	81.119(3)
γ/°	90.0	76.369(3)
Volume/Å^3	2040.5(5)	1419.0(1)
Z	4	2
Density (calcd)/g cm^{-3}	1.392	1.892
Absorption coefficient/mm^{-1}	0.195	1.521
F(000)	904	808
Diffractometer	Bruker SMART-CCD	Bruker SMART-CCD
Temperature/K	150.0(2)	101.5(2)
Radiation, λ/Å	Graphite monochromatized MoK_α (0.71073)	Graphite monochromatized MoK_α (0.71073)
Scan mode, scan step/°	ω, 0.3	ω, 0.3
Time per step/s	15	15
Theta range/°	1.43 to 28.00	1.53 to 28.00
Index ranges	$-6 \leqslant h \leqslant 7$, $-19 \leqslant k \leqslant 19$, $-38 \leqslant l \leqslant 36$	$-12 \leqslant h \leqslant 11$, $-16 \leqslant k \leqslant 16$, $-18 \leqslant l \leqslant 18$
Reflections collected	17 287	15 682
Independent reflections	4934 [R(int) = 0.0921]	6809 [R(int) = 0.0782]
Absorption correction	Empirical (SADABS)	Empirical (SHELXTL-Plus)
Min. and max. transmission	0.526520 and 1.00000	0.74396 and 0.84117
Data/restraints/parameters	4117/0/410	5997/0/501
Goodness-of-fit on F^2	1.005	1.002
Final R indices [$I > 2\sigma(I)$]	$R_1 = 0.0522$, $wR_2 = 0.1046$	$R_1 = 0.0532$, $wR_2 = 0.1044$
R indices (all data)	$R_1 = 0.1213$, $wR_2 = 0.1372$	$R_1 = 0.1027$, $wR_2 = 0.1258$
Extinction coefficient	0.006(1)	0.0000(3)
Largest diff. peak and hole, e Å^{-3}	0.489 and −0.200	1.159 and −0.690

Bruker SMART-CCD diffractometer (Mo-K_α radiation, ω scan mode, 0.3° frame, 15 s per frame, 150.0 K for **1** and 110.0 K for **2**). Structures of **1** and [**1**·$(Ag^+)_2$] were solved by direct methods and refined by full-matrix least-squares on F^2. The solution of structure **1** led to two disordered positions of the central fragment in the vicinity of the ethylene group and thiazole ring. The refinement of the structure was performed by using the instruction "part" and free variable for occupation factor of the disordered fragment. Both disordered positions have approximately equal site occupation factors (s.o.f. ~ 0.5). Further refinement was performed in anisotropic approximation for all non-hydrogen atoms, isotropic approximation for the hydrogen atoms not included in the disordered fragment, and using the "riding" model for the hydrogen atoms of the disordered fragment. To check the possibility for the double unit cell to occur, we processed the experimental data for the double unit cell ($a = 10.114$ Å, $V = 4081.0$ Å^3) although reflections with odd h were lacking. In this case, the same type of disordering was observed on structure solution and refinement.

Structure [**1**·$(Ag^+)_2$] was refined in anisotropic approximation for all non-hydrogen atoms. The hydrogen atoms were located from difference Fourier synthesis and refined using the "riding" model for all hydrogen atoms except those of the acetonitrile ligand. The last named atoms were refined in the isotropic approximation.

SHELXS-86[14] and SHELXL-93[15] were used for structure solution and refinement, respectively.

CCDC reference numbers 185189 and 185190. See http://www.rsc.org/suppdata/nj/b2/b205305e/ for crystallographic data in CIF or other electronic format.

Acknowledgements

The study was supported by CRDF (Grant RC2-2344-MO-02), RFBR (Project Nos. 00-03-32159, 00-03-32898, 01-03-32474, 01-03-32757 and 02-03-33058). Financial support from the Royal Society of Chemistry (RSC Journal Grants for International Authors for A.V.C. and L.G.K.), the EPSRC for a Senior Research Fellowship (J.A.K.H.) and Ministry for Science and Technologies of Russia is gratefully acknowledged.

References

1 (*a*) *Applied fluorescence in chemistry, biology, and medicine*, eds. W. Rettig, B. Strehmel, S. Schrader and H. Seifert, Springer-Verlag, Berlin, 1999; (*b*) G. G. Guilbault, *Practical Fluorescence. Theory, Methods and Techniques*, M. Dekker, New York, 1973; (*c*) B. M. Krasnovskii and B. M. Boilotin, *Organic Luminescence Materials*, VCH, Weinheim, 1988; (*d*) S. G. Schulman, *Molecular Luminescence Spectroscopy. Methods, Application*, John Wiley, Chichester, 1993; (*e*) T. G. Dewey, *Biophysical and Biochemical Aspect of Fluorescence Spectroscopy*, Plenum, New York, 1991; (*f*) M. C. Goldberg, *Luminescence Application in Biological, Chemical Environmental and Hydrological Sciences*, ACS Symp. Ser. vol. 383, Am. Chem. Soc., Washington, DC, 1989; (*g*) I. F. Hemmila, *Application of Fluorescence in Immunoassays*, Marcel Dekker, New York, 1991; (*h*) B. Valeur and I. Leray, *Coord. Chem. Rev.*, 2000, **205**, 3.

2 (*a*) K. Rurack, W. Rettig and U. Resch-Gerger, *Chem. Commun.*, 2000, 407–408; (*b*) K. Rurack, M. Sczepan, M. Spieles, U. Resch-Gerger and W. Rettig, *Chem. Phys. Lett.*, 2000, **320**, 87–94; (*c*) Y. L. Bricks, J. L. Slominskii, M. F. Kudinova, A. I. Tolmachev, K. Rurack, U. Resch-Gerger and W. Rettig, *Photochem. Photobiol. A*, 2000, **132**, 193; (*d*) J. Bourson and B. Valeur, *J. Phys. Chem.*, 1989, **93**, 3871; (*e*) M. M. Martin, P. Plaza, N. D. Hung, Y. H. Meyer, J. Bourson and B. Valeur, *Chem. Phys. Lett.*, 1993, **202**, 425; (*f*) S. Fery-Forgues, J. Bourson, L. Dallery and B. Valeur, *New J. Chem.*, 1990, **14**, 617; (*g*) L. Cazaux, M. Faher, A. Lopez, C. Picard and P. Tisnes, *J. Photochem. Photobiol. A: Chem.*, 1994, **77**, 217; (*h*) L. Cazaux, A. Lopez and C. Picard, *Can J. Chem.*, 1993, **71**, 2007.

3 (*a*) A. V. Barzykin, M. A. Fox, E. N. Ushakov, O. B. Stanislavsky, S. P. Gromov, O. A. Fedorova and M. V. Alfimov, *J. Am. Chem. Soc.*, 1992, **114**, 6381; (*b*) S. I. Druzhinin, M. V. Rusalov, B. M. Uzhinov, M. V. Alfimov, S. P. Gromov and O. A. Fedorova, *Proc. Indian Acad. Sci. (Chem. Sci.)*, 1995, **107**, 721; (*c*) S. P. Gromov, E. N. Ushakov, O. A. Fedorova and M. V. Alfimov, *Russ. Chem. Bull.*, 1997, **46**, 463; (*d*)) S. P. Gromov, E. N. Ushakov, O. A. Fedorova, V. A. Soldatenkova and M. V. Alfimov, *Russ. Chem. Bull.*, 1997, **46**, 1143; (*e*) M. V. Alfimov and S. P. Gromov, *Applied fluorescence in chemistry, biology, and medicine*, eds. W. Rettig, B. Strehmel, S. Schrader and H. Seifert, Springer-Verlag, Berlin, 1999, p. 161.

4 A. Dondoni, G. Fantin, M. Fogagnolo, A. Medici and P. Pedrini, *Tetrahedron*, 1988, **44**, 2021.

5 F. Wada, H. Hirayama, H. Namiki, K. Kikukawa and T. Matsuda, *Bull. Chem. Soc. Jpn.*, 1980, **53**, 1473.

6 S. P. Gromov, O. A. Fedorova, M. V. Fomina, M. V. Alfimov, *RF Pat.* 2012574, 1994.

7 M. Koral, D. Bonis, A. J. Fusco, P. Dougherty, A. Leifer and J. E. LuValle, *J. Chem. Eng. Data*, 1964, **9**, 406.

8 M. Shirai, T. Orikata and M. Tanaka, *J. Polym. Sci.: Polym. Chem. Ed.*, 1985, **23**, 463.

9 P. Gans, A. Sabatini and A. Vacca, *Talanta*, 1996, **43**, 1739.

10 (*a*) B. Valeur and I. Leray, *Coord. Chem. Rev.*, 2000, **205**, 3; (*b*) W. Rettig and R. Lapouyarde, in *Topics in Fluorescence Spectroscopy*, ed. J. R. Lakowics, Plenum, New York, 1994, vol. 4, p. 109; (*c*) B. Valeur, F. Badaoui, E. Bardez, J. Bourson, P. Boutin, A. Chatelein, I. Devol, B. Larrey, J. P. Lefevre and A. Soulet, in *Chemosensors of ion and molecular recognition*, ed. J.-P. Desvergne and A. W. Czarnik, NATO ASI Series, Kluwer, Dordrecht, 1977; (*d*) I. I. Baskin, K. Ya. Burstein, A. A. Bagatur'yants, S. P. Gromov and M. V. Alfimov, *J. Mol. Struct.*, 1992, **274**, 93; (*e*) S. P. Gromov, D. E. Levin, K. Ya. Burstein, V. A. Krasnovskii, S. N. Dmitrieva, A. A. Golosov and M. V. Alfimov, *Russ. Chem. Bull.*, 1997, **46**, 959.

11 A. A. Bagatur'yants, A. Ya. Freidzon, M. V. Alfimov, E. J. Baerends, K. A. K. Howard, L. G. Kuz'mina, *J. Mol. Struct. (Theochem.)*, 2002, in press.

12 F. H. Allen and O. Kennard, *Chem. Des. Automat. News*, 1993, **8**, 1.

13 G. Weber and F. W. J. Teale, *Trans. Faraday Soc.*, 1957, **53**, 646.

14 G. M. Sheldrick, *Acta Crystallogr., Sect. A*, 1990, **46**, 467–473.

15 G. M. Sheldrick, SHELXL-93 - Program for the Refinement of Crystal Structures, University of Göttingen, Germany, 1997.